Body Movement Activity Recognition for Ambulatory Cardiac Monitoring

Tanmay Pawar*, Subhasis Chaudhuri, *Senior Member, IEEE*, and Siddhartha P. Duttagupta, *Member, IEEE*

***Abstract*—Wearable electrocardiogram (W-ECG) recorders are increasingly in use by people suffering from cardiac abnormalities who also choose to lead an active lifestyle. The challenge presently is that the ECG signal is influenced by motion artifacts induced by body movement activity (BMA) of the wearer. The usual practice is to develop effective filtering algorithms which will eliminate artifacts. Instead, our goal is to detect the motion artifacts and classify the type of BMA from the ECG signal itself. We have recorded the ECG signals during specified BMAs, e.g., sitting still, walking, movements of arms and climbing stairs, etc. with a single-lead system. The collected ECG signal during BMA is presumed to be an additive mix of signals due to cardiac activities, motion artifacts and sensor noise. A particular class of BMA is characterized by applying eigen decomposition on the corresponding ECG data. The classification accuracies range from 70% to 98% for various class combinations of BMAs depending on their uniqueness based on this technique. The above classification is also useful for analysis of P and T waves in the presence of BMA.**

***Index Terms*—Artifact removal, body movement activity, classification, ECG, wearable systems.**

I. Introduction

In the situation where dynamic monitoring of heart is required, a light-weight, wearable electrocardiogram recorder (W-ECG) may prove to be a more convenient option compared to the standard Holter monitor which often restricts free movement of the person. Further, in a developing country such as India, where the number of people with cardiac abnormalities is expected to grow significantly, affordability and availability are also critical. At IIT Bombay we are focused on developing low cost ambulatory ECG solutions. For this purpose we have used a W-ECG with an inbuilt data acquisition system developed by Lal *et al.* [1]. The W-ECG is a single-lead system, which is unrestrictive and convenient from a user standpoint (see Fig. 1). It can store up to 48 hours long recording of the signal which can be downloaded to a personal computer via a serial port.

For ambulatory ECG recorders the impact of body movement activity (BMA) on motion artifacts has not been fully investigated. The goal of this paper is to study motion artifacts in the ECG signal in order to improve accuracy of the W-ECG and similar ambulatory ECG recorders that are commercially available. Currently, we have restricted our studies to only people with no known cardiac abnormalities but at multiple settings (laboratory and outdoors). Subsequently, we plan to test on actual patients also at all locations.

Fig. 1. A picture of the W-ECG developed at IIT Bombay, placed by the side of a 15-cm ruler.

The ECG signal collected by the W-ECG is corrupted by BMA induced artifacts owing to disturbances in skin-electrodes interface and noise due to muscular activities, collectively known as motion artifacts. For the W-ECG, to handle motion artifacts occurring naturally during its intended use is a challenge. The motion artifacts have a significant overlap in frequency with ECG signal, so filtering based on spectral separation is of limited use [2]. Since BMA influences the ECG output, we propose to determine the BMA from the motion artifacts in the ECG signal. This will be helpful eventually in dynamic monitoring of cardiac activity of a patient and determining if any BMA is having a deleterious effect. Determination of the BMA from ECG data is yet to be fully studied in the literature. The possibility of such a classification was initially explored in [3]. In [3], the ECG signals were analyzed using wavelet transform and a neural network. The signatures of 3 typical movement patterns were extracted by characterizing the low frequency artifacts. However, the reported performance is not very satisfactory as the wavelet based representation does not separate the in-band BMA signal from the ECG. In other works related to BMA analysis from nonambulatory ECG, body position changes are detected for ischemia monitoring in [4]–[6]. In [4], [6], Karhunen–Loeve transform features of the ECG beats are analyzed to detect position changes. A synthesized vectorcardiograph based approach has been proposed in [5], [6], where a series of angles for the three orthogonal leads X, Y and Z are derived using a loop alignment method [5], [7]. The angle series is then analyzed to detect the body position changes. However, this method requires a comprehensive 12-lead ECG signal to be able to synthesize

Manuscript received April 27, 2006; revised October 1, 2006. This work was supported in part by the Swarnajayanti Fellowship. A preliminary version of the manuscript dealing with single person training has earlier been presented at the Engineering in Medicine and Biology Conference (EMBC), 2006. *Asterisk indicates corresponding author.*

*T. Pawar is with the Department of Electrical Engineering, Indian Institute of Technology-Bombay, Mumbai 400076, India (e-mail: tanmaypawar@iitb.ac.in).

S. Chaudhuri and S. P. Duttagupta are with the Department of Electrical Engineering, Indian Institute of Technology-Bombay, Mumbai 400076, India (e-mail: sc@ee.iitb.ac.in; sdgupta@ee.iitb.ac.in).

Color versions of one or more of the figures in this paper are available online at http://ieeexplore.ieee.org.

Digital Object Identifier 10.1109/TBME.2006.889186

the three vectorcardiograph leads and is currently restricted to nonambulatory BMA. The single lead system that we have used will be less informative but will enable monitoring of a range of BMAs and will also be preferable from the standpoint of wearer comfort and cost.

In this paper we characterize the motion artifacts induced by the following BMAs: sitting still, up and down movement of left, right and both arms, walking on a level floor, and climbing stairs up and down, using a supervised learning approach based on principal component analysis (PCA). We then test for classifiability of the motion artifacts based on this characterization. For this, we build various BMA classifiers for different BMA classes where each class is either a distinct BMA or a combination of two or more different BMAs as specified above. If two specified BMAs are not quite separable using the proposed characterization of motion artifacts, they are both combined into a single BMA class. In this report we demonstrate that it is indeed possible to recognize several BMA classes accurately from the ECG signal itself. Since the above classification is based on the PCA of motion artifacts in the ECG signal, it follows that class specific PCA-filtering can also be used for removal of motion artifacts. Accordingly, we have demonstrated the usefulness of the PCA-filtering technique by locating the P and T waves in the ECG signal in the presence of body movement.

The organization of the paper is as follows. The set of specified type of BMAs that are prevalent in our daily life, and the data acquisition procedure are described in Section II. A mathematical model for representation of the ECG signal recorded by the W-ECG is explained in Section III. The proposed BMA classification algorithm is given in Section IV. Here, we also explain how the BMA classification can be used for removal of the motion artifacts. The results of the classification algorithm for various types of BMA classes and P and T-wave detection in presence of BMA are presented in Section V. The conclusions are noted in Section VI.

II. Data Acquisition

The specifications of the W-ECG are as follows: single lead, bandwidth- 0.28 to 106 Hz, sampling frequency- 256 Hz, analog-to-digital conversion (12 bits/sample) [1]. The lead-II configuration [8] is chosen for all the recordings in this study for consistency. In this experiment, commonplace BMAs such as sitting, walking, movement of arms, and climbing up and down stairs are recorded. Stair climbing is chosen as it is a routine activity in urban life, especially in India. The activities are performed over short duration followed by sufficient rest so that the effect of a particular BMA subsides before the next data set is collected. Thus, care has been taken not to unduly stress the heart during the BMA. Since climbing up the stairs may cause stress, this is restricted to only up to three floors and is performed at a relaxed pace. Finally, we are exploring the feasibility of BMA recognition from a single-lead W-ECG, thus, as a precaution, testing is restricted to subjects with no known cardiac problems. The following are the different BMAs considered in our study:

1) sitting still on a chair;
2) up and down movement of left arm, at a rate of approximately 25 cycles of the up-down movement per minute;
3) up and down movement of right arm, at a similar pace;
4) similar up and down movement of both arms;
5) walking at a gentle pace with an average speed of about 3 km/hour on a level floor;
6) twisting left-right-left body movement at the waist while standing at a rate of approximately 25 cycles per minute, as a common body stretching activity;
7) climbing down stairs at an average rate of 100 steps per minute or equivalently coming down at an average speed of 30 cm/s;
8) climbing up stairs at an average rate of 85 steps per minute or equivalently gaining a height at an average speed of 25 cm/s.

A total of 23 healthy subjects were chosen in the age group of 22–50 years with an average age of 29 years and a standard deviation of 7 years. All subjects were intentionally chosen to be right-handed males in order to preclude variations arising out of possible gender and orientation effects. In addition, there were no instances of dextrocardia. The subjects volunteered to perform all of the above defined classes of body movement. A part of the data collected was used for training purposes and the other part was reserved for performance evaluation of the proposed technique. The ground truth with regards to type of BMA is known for the entire dataset.

III. Mathematical Model

The ambulatory ECG signal recorded in this experiment has three components: cardiac signal due to normal heart activity, motion artifacts due to body movement and sensor noise introduced by the W-ECG. Following [3], we hypothesize that each type of body movement induces a particular type of motion artifacts in the ECG signal. An ECG signal for the i^{th} class of BMA is modeled as

$$r_i(n) = q_i(n) + s_i(n) + \eta(n) \tag{1}$$

where r_i is a recorded ECG signal, q_i is a cardiac signal of a normal heart, s_i is an additive motion artifact due to i^{th} class of BMA and η is the sensor noise present in the ECG signal.

Let the vector representations of the corresponding signals captured during a single period of heart beat be $\underline{r}_i$, $\underline{q}_i$, $\underline{s}_i$ and $\underline{\eta}$, respectively. All vectors used in this paper are column vectors. The dimension M_0 of these vectors depend on the beat period and the sampling frequency. For example, for a normal heart rate of 72/min and sampling rate of 256 Hz, the dimension $M_0 = 256 \times 60/72 \approx 213$. If one considers N consecutive heartbeats together as a signal then the dimension of the signal would be NM_0. Following are the critical assumptions made while developing a classifier.

1) The cardiac signal q_i is assumed to be representing normal cardiac activity only and it remains stable in the presence of specific BMA for a duration of 1 min.
2) Since cardiac activity is by nature involuntary, it is independent of voluntary muscular activities and motion of electrodes. Hence motion artifacts s_i caused by these factors are independent of the cardiac signal q_i, i.e., $q_i \perp s_i$.

3) The sensor noise η present in the ECG signal is due to ambient conditions of recording like power line interference, device temperature, skin humidity, etc. and, therefore, it is assumed to be independent of both cardiac signal and the motion artifact, i.e., $\eta \perp q_i$ and $\eta \perp s_i$.
4) In the preprocessing steps described next (Section IV), the dc bias estimated from the isoelectric level of the ECG signal is set to zero. Therefore, the sensor noise is assumed to be of zero mean, i.e., $E[\underline{\eta}] = 0$.
5) $\mathrm{Rank}(E[\underline{r}_i \underline{r}_i^T]) \approx M_i$, where $M_i \leq M_0$, signifying that the actual information in the recorded ECG signal can be compactly represented by only top M_i eigenvectors.
6) The energy of the motion artifact signal s_i is concentrated into a top few (say K_i where $K_i \ll M_i$) eigenvectors of $E[\underline{s}_i \underline{s}_i^T]$, and that the composite signal $\underline{r}_i$ is sufficiently excitatory.
7) There is greater correlation between signals due to same type of body movement than that for any two different types of body movement. That is, s_i and s_k are highly correlated if $i = k$ (at different time instants) and nearly uncorrelated if $i \neq k$.
8) The signal component due to motion artifacts is smaller compared to the strength of the cardiac signal, but much greater than the sensor noise, i.e., $|\underline{\eta}| \ll |\underline{s}_i| < |\underline{q}_i|, \forall i$.

IV. Experimental Methods

Based on the mathematical model discussed in the previous section, we propose to extract the signature of a specific BMA (s_i) by eliminating the cardiac signal (q_i) and the sensor noise (η). In essence, we are studying what is normally termed as motion artifacts or part of the "noise" in the ECG data due to specific types of body movement.

The cardiac signal is characterized by a stable rhythm of heart beats. Following assumption III.1, the cardiac rhythm stays nearly constant over the heart beats within the observation window. An arithmetic mean of several epochs of heart beats will provide the best estimate of the constant cardiac rhythm and hence the cardiac signal [2], [9]. For a specific BMA class, this estimate is averaged over the entire training data set for a particular class and is termed as class-mean of the BMA. If the class-mean is a correct estimate of the cardiac signal then according to (1), the motion artifacts component (also sensor noise) is derived by removing the class-mean from the ECG signal.

The sensor noise component is suppressed by elimination of the dc bias during the preprocessing step described next. Accordingly, the motion artifacts component will dominate as per assumption III.8.

In the proposed method, an unknown ECG beat is classified into a specific BMA class according to the best reconstruction criterion. A particular BMA class is represented by a set of the top few eigenvectors of the training BMA data belonging to that BMA class. The eigenvectors are derived by eigen decomposition of the correlation matrix of the training BMA data. The test ECG beat is reconstructed using the set of eigenvectors in conjunction with the class-mean for each BMA class. The BMA class for which the distance between the reconstructed signal and the test ECG beat is minimum is determined as the true BMA class for the unknown ambulatory ECG data.

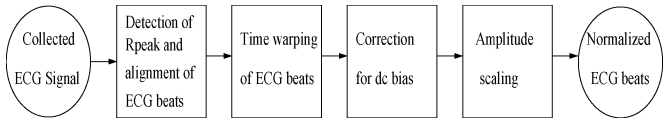

Fig. 2. Preprocessing applied to the captured ECG signal by the W-ECG.

The eigen decomposition technique described above is optimal for the assumed data representation model because the eigenvectors are orthogonal. Thus, after preprocessing, if the artifact signal (s_i) is corrupted by an uncorrelated noise signal (η) then the top few eigenvectors will represent mostly the signal component due to BMA as the signal to noise ratio (SNR) will be high in these components and the remaining eigenvectors will mostly represent the noise subspace, thus isolating the BMA signal from noise.

Thus, the proposed method is a supervised technique for body movement classification. However, in order to be able to use the technique and for suppressing the sensor noise η, certain preprocessing steps are required to handle both intrapersonal and interpersonal variations in the cardiac signal (q_i).

A. Preprocessing of ECG Data

It is assumed that the heart is not stressed during the BMAs that are being performed in this study. However, certain parameters like the coupling between skin and electrodes, and the variability of the heart rate are beyond our control. The coupling between skin and electrodes depends mostly on the skin humidity levels and also if the setting is indoors or outdoors. Similarly, a small variation of heart rate during ambulatory activity is considered quite normal. Finally, there are interpersonal variations in the above two parameters. While the coupling between skin and electrodes affects the amplitude (scale) of the ECG beat data, the heart rate affects the time interval of the ECG beat data.

The arithmetic mean estimate of the cardiac signal $(\underline{q}_i)$ and eigen decomposition for extraction of the motion artifact component $(\underline{s}_i)$ are both sensitive to translation, variations in amplitude and time scales of the data [4]. Thus, it is necessary to perform the following preprocessing steps that involve proper alignment, amplitude scaling and time warping of the data as shown in Fig. 2.

The data is processed as a batch of ECG beat epochs collected over a 1-min duration. This is considering that all the epochs have the same amplitude scale and are of the same duration.

1) Detection of R-Peak and Alignment of ECG Beats: The R-peak is the most prominent feature of the ECG signal that can be detected easily even in presence of motion artifacts, and is used for calculating the heart rate. The R-peaks in the ECG signals are detected using the Pan-Tompkins method [10]. The duration between the current R-peak and the one prior to it is considered as the current ECG beat interval, i.e., j^{th} beat interval is given by duration between $(j-1)^{th}$ and j^{th} R-peaks. The average interval of the ECG beats is estimated from the number of detected R-peaks within a 1-min duration. The ECG signal is then partitioned into N average interval wide ECG beat epochs. The R-peak in each epoch is aligned to the exact middle

position. This strategy ensures the alignment of ECG beats even after time warping is applied to the data.

2) Time Warping of ECG Beats: As explained above, the ECG beat intervals may vary due to change in the heart rate. Accordingly, for a fixed sampling rate, the number of samples recorded for each ECG beat interval will also vary. Since the proposed method, based on arithmetic mean calculation and eigen analysis of vectors, is applicable only to vector observations in a space of fixed dimension, it is required to equalize the dimensions (M_0) of all the ECG beats. A simple technique to achieve this is linear time warping and is implemented as follows. The ECG beat is resampled by a rational factor a/b, where a is the fixed number of samples after the time warping, and b is the number of samples in the ECG beat being resampled. This is performed through MATLAB using a polyphase implementation of resampling and linear phase anti-aliasing filter with finite impulse response. Following application of time warping, all the ECG beat observations are of equal length.

3) Correction for dc Bias: The constant voltage level of the flat ECG beat segment that lies between the end of P wave and the beginning of Q wave is termed the isoelectric level of the ECG beat [9]. Ideally, the isoelectric level should be at ground potential. The dc bias is estimated by calculating the arithmetic mean of isoelectric levels of all ECG beat observations collected during a 1-min interval. This dc bias is then subtracted from the ECG signal. Thus, any dc bias introduced due to sensor noise or otherwise is removed during this step. The shape of the recorded ECG signal remains unchanged at this point of time and the sensor noise in ECG signal has now zero mean as per assumption III.4.

4) Amplitude Scaling: This is the last stage of preprocessing. As discussed earlier, the coupling between skin and electrodes can affect the amplitude of the signal. Since the proposed method calculates the arithmetic mean of the ECG beats for estimating the cardiac signal component, all the ECG beats should represent the cardiac activity with the same amplitude. The R-wave peak with respect to the isoelectric level is considered here to represent the full signal strength. A normalization factor is estimated by averaging of R-wave amplitudes with respect to the corresponding isoelectric levels from all ECG beats over a period of 1 min. Thus, the amplitude of the ECG data over the period is normalized and the average estimate of R-wave amplitude is unity.

B. Supervised Learning of Body Movement

The ECG signal now comprises of the cardiac signal (q_i), motion artifacts (s_i) and sensor noise (η) which has been suppressed through preprocessing, and is considered for training and subsequent classification of BMA. As explained in Section III, the vector representation of the j^{th} ECG beat observation in the training data of i^{th} BMA class is $\underline{r}_{ij}$ and the vector representations of the corresponding cardiac signal, motion artifact and sensor noise components are $\underline{q}_{ij}$, $\underline{s}_{ij}$ and $\underline{\eta}_{ij}$, respectively.

We propose a supervised approach of training a BMA classifier using the processed ECG beat observations, $\underline{r}_{ij}$, $i = 1, 2, \ldots, c$ and $j = 1, 2, \ldots, N_i$, where c is the number of BMA classes in a classifier and N_i is the number of ECG beat observations used for training of i^{th} BMA class. In this approach each BMA class is represented by a class-mean vector and a set of eigenvectors computed using the PCA of all training observations. First, the class-mean is simply the arithmetic mean of the training data $\underline{r}_{ij}$, $j = 1, 2, \ldots, N_i$ of the i^{th} BMA class. The eigenvectors for the BMA class are extracted from the corresponding data after subtracting the class-mean.

The class-mean of i^{th} BMA class is calculated as follows

$$\widetilde{\underline{q}}_i = \frac{1}{N_i} \sum_{j=1}^{N_i} (\underline{r}_{ij}) \tag{2}$$

which approximates the average cardiac signal for the given BMA class [9]. The average cardiac component $\widetilde{\underline{q}}_i$ is subtracted from the signal $\underline{r}_{ij}$ to derive mean-subtracted BMA vectors (residual signal) for the i^{th} BMA class

$$\underline{r'}_{ij} = \underline{r}_{ij} - \widetilde{\underline{q}}_i = \underline{s}_{ij} + \underline{\eta'}_{ij} \tag{3}$$

where $\underline{\eta'}_{ij}$ is comprised of the sensor noise plus the noise arising in the estimation of the cardiac component due to interpersonal variation (refer to multi-subject testing, classifiers VI-X in Section V). The BMA vectors with regards to signal power, contain predominantly the motion artifact $\underline{s}_{ij}$, along with the noise $\underline{\eta'}_{ij}$.

Next, PCA is applied on the BMA vectors $\underline{r'}_{ij}$ to compute the significant eigenvectors of the training data of each BMA class. An eigenvalue corresponding to an eigenvector is a measure of signal strength in the data in the direction of the eigenvector. Since as per assumption III.8, the motion artifact component is dominating in the residual signal, if the eigenvectors of this data are arranged in nonascending order of the respective eigenvalues, the first few eigenvectors will represent the motion artifacts by neglecting the noise components. For the i^{th} BMA class, the eigenvectors and eigenvalues are computed by eigen decomposition of a covariance matrix of the training residual signal $\underline{r'}_{ij}$ given by

$$C_i = \frac{1}{N_i} \sum_{j=1}^{N_i} \left(\underline{r'}_{ij}\right) \left(\underline{r'}_{ij}\right)^T \tag{4}$$

where C_i is the covariance matrix for the i^{th} BMA class and $(\cdot)^T$ is matrix transpose. If the data occupies an M dimensional space then C_i is a $M \times M$ matrix and its eigen decomposition gives a total M eigenvectors $[e_{i1}, e_{i2}, \ldots, e_{iM}]$, arranged in nonascending order of the corresponding eigenvalues denoted by $\lambda_{i1} \geq \lambda_{i2} \geq \ldots \geq \lambda_{iM}$ for the i^{th} BMA class. Let $E_i = [e_{i1}, e_{i2}, \ldots, e_{iK_i}]$, $K_i \ll M$ be a set of first K_i eigenvectors with the highest eigenvalues that represent the motion artifacts. Here, E_i forms a basis for a small K_i dimensional motion artifact subspace in the M dimensional space of the data for the i^{th} class. Since as per assumption III.7 the motion artifacts due to any two different types of BMA are nearly uncorrelated, eigen functions for any two different motion artifacts are also expected to be nearly uncorrelated.

For each BMA class, a class-mean and a set of eigenvectors are computed from the training observations, which represent the characteristics of motion artifacts for the particular BMA and is used as the basis of the BMA classifier.

C. Body Movement Classification

The proposed BMA classification procedure is presented here. Let $\underline{p}_u$ be a test ECG beat extracted after the preprocessing steps given in Section IV-A, where u is the label of the BMA class of $\underline{p}_u$ which is unknown to the BMA classifier but can be any one of BMA class labels $i = 1, 2, \ldots, c$; where c is the total number of BMA classes in the classifier. To classify $\underline{p}_u$, i.e., to recognize the class label u, the following procedure is applied. First, the class-mean $\widetilde{\underline{q}}_i$ is subtracted from $\underline{p}_u$ for all the BMA classes $i = 1, 2, \ldots, c$ to get

$$\underline{p'}_i = \underline{p}_u - \widetilde{\underline{q}}_i \tag{5}$$

where $\underline{p'}_i$ is a mean-subtracted residual BMA vector for the i^{th} BMA class. The BMA vector $\underline{p'}_i$ is reconstructed from projections on the computed set of eigenvectors E_i to capture its contents in the i^{th} motion artifact subspace defined by E_i in the prior training as

$$\widetilde{\underline{p'}}_i = \left(E_i E_i^T\right) \underline{p'}_i \tag{6}$$

where $\widetilde{\underline{p'}}_i$ is the reconstructed i^{th} motion artifact.

A measure of error in the reconstruction in i^{th} motion artifact is denoted by $error(i)$ and defined as

$$error(i) = \left| \widetilde{\underline{p'}}_i - \underline{p'}_i \right|^2. \tag{7}$$

To recognize the BMA class of the ECG beat, u is assigned the class label from $i = 1, 2, \ldots, c$ for which the error in reconstruction is the minimum

$$u = \arg\min_i error(i). \tag{8}$$

The above derivation is valid when one is trying to classify motion artifacts using the ECG signal for a single beat duration. However, one can have l number of consecutive ECG beats during a particular BMA. The use of l beats instead of a single beat can lead to a better classification accuracy. Hence, for the BMA classifier, the proposed method of classification can be generalized for a sequence of l test ECG beats $\{p\}_u = \{\underline{p}_{u1}, \underline{p}_{u2}, \ldots, \underline{p}_{ul}\}$, where $\underline{p}_{uj}$ is j^{th} test ECG beat and u is the single label for all the test ECG beats in the sequence. The error in reconstruction given in (7) for the test ECG beats $\underline{p}_{uj}$, is denoted by $error_j(i)$ for $j = 1, 2, \ldots, l$ in the given sequence. Finally, the following measure of error is computed

$$error(i) = \sum_{j=1}^{l} error_j(i). \tag{9}$$

The class label corresponds to i for which $error(i)$ is minimum.

D. Artifact Removal

The classification procedure as derived above can also be applied to eliminate motion artifacts in ECG due to body movements. The BMA class for an ECG beat under test is recognized by the BMA classifier and the corresponding artifact components are removed. Let $\underline{p}_i$ be an ECG beat where i is the recognized BMA class, and the set of eigenvectors E_i represents the artifacts in $\underline{p}_i$ due to the recognized BMA. For artifact removal, the ECG beat is reconstructed by removing the components of the corresponding mean subtracted observation $\underline{p'}_i = \underline{p}_i - \widetilde{\underline{q}}_i$, in the artifact subspace spanned by E_i as

$$\widetilde{\underline{p}}_i = \underline{p}_i - \left(E_i E_i^T\right) \underline{p'}_i \tag{10}$$

where $\widetilde{\underline{q}}_i$ is the class-mean of the recognized BMA class as defined in (2) and $\widetilde{\underline{p}}_i$ is the reconstructed ECG beat.

V. Results

A. BMA Classification

A uniform length of 160 sample point duration is chosen for each ECG beat during the preprocessing steps. The BMA label (ground truth) is known for each of the ECG beats collected. The data set is divided into two parts: one for training the classifiers and the other for classifier testing purposes. The exact details of the population size for each of these two parts for various BMA are given in Table I. The column "Single Subject" corresponds to the case where the classifier is trained for a particular subject (subject number one in our experiment) and tested on the same subject. The last column corresponds to the case when the classifier is both trained and tested for a collective pool of subjects and not specific for a single subject. The known BMA labels in the test data are used for performance evaluation of the classifier testing and are not available to the classifier itself. The classification test is performed on the sequences of 30 ECG beats (30 $\times$ 160 sample points).

The performance is evaluated based on two parameters: accuracy (P_T) defined as

$$P_T = N_{\text{true}}/(N_{\text{true}} + N_{\text{missed}}) \tag{11}$$

and false detection rates (P_F) defined as

$$P_F = N_{\text{false}}/(N_{\text{true}} + N_{\text{false}}) \tag{12}$$

where N_{true} is the number of true detections, N_{missed} is the number of missed detections and N_{false} is the number of false detections.

For example, a classifier has three classes namely A1, A2 and A3 and the corresponding number of test signals recorded are 100, 90 and 80. Now, if the classifier detects 95 test signals as class A1 and 10 out of these 95 detections, actually belong to either class A2 or class A3 rather than class A1, then $N_{\text{false}} = 10$, $N_{\text{true}} = 95 - 10 = 85$ and $N_{\text{missed}} = 100 - 85 = 15$.

TABLE I
DETAILS OF NUMBER OF ECG BEATS USED FOR TRAINING AND TESTING OF A PARTICULAR BMA

Body movement activity	Single Subject		Multiple Subjects	
	training	testing	training	testing
Sitting still	289	578	2927	5854
Left arm	227	454	2336	4672
Right arm	278	557	2278	4556
Both arms	224	449	1586	3112
Walking	583	1167	4120	8240
Twisting	355	711	2798	5597
Climbing down	268	536	1407	2814
Climbing up	344	688	1879	3759
Total	2568	5140	19331	38604

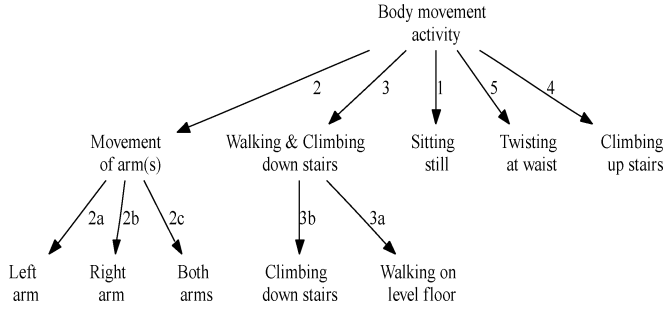

Fig. 3. Various BMAs and possible class formation by combining two or more BMAs into a single class.

TABLE II
FIVE DIFFERENT CLASSIFIERS FOR SUBJECT SPECIFIC TRAINING WITH VARIOUS COMBINATIONS OF BMA CLASSES/SUBCLASSES IN FIG. 3. THE CORRESPONDING CLASSIFIERS FOR MULTIPLE SUBJECTS ARE VI TO IX. THE CLASSIFIER X DEALS WITH TOTALLY UNKNOWN SUBJECTS

Classifier	BMA
I, VI, X	1, 2, 3 and 4
II, VII	1, 2, 3a, 3b and 4
III, VIII	1, 2a, 2b, 2c, 3 and 4
IV, IX	1, 2a, 2b, 2c, 3a, 3b and 4
V	1, 2a, 2b, 2c, 3a, 3b, 4 and 5

A hierarchical tree structure of BMA classes is shown in Fig. 3. There are five BMA classes in the top layer: 1) sitting still; 2) arm movement; 3) walking and climbing down stairs (W&Cd); 4) climbing upstairs; 5) twisting movement at waist. The arm movement is a combined class of three separate movements of 2a) left arm, 2b) right arm, and 2c) both arms. Similarly, W&Cd is a combination of two BMA subclasses: 3a) walking; 3b) climbing down stairs. These BMA subclasses, shown in the second layer of the graph, demonstrate significant correlation among the corresponding motion artifacts. As a result these subclasses are subject to false detections. To study this aspect of BMA classification in ECG signals, we construct five different types of BMA classifiers (Table II) formed by various possible combinations of BMA classes/subclasses (Fig. 3).

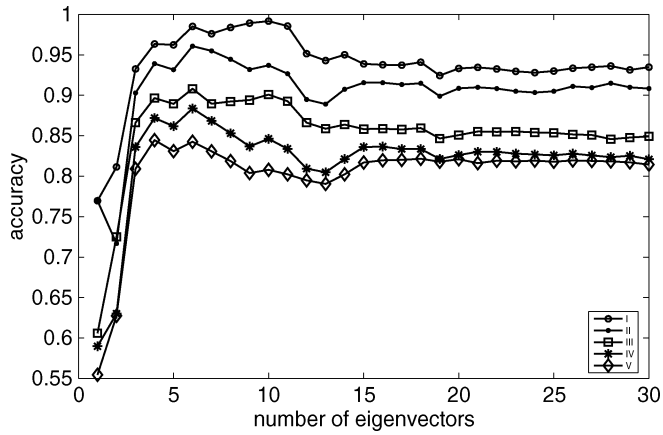

Fig. 4. Classification accuracy as a function of number of eigenvectors for the BMA classifiers: I–V.

Since an artifact subspace in the proposed scheme of BMA classification is represented by a corresponding set of eigenvectors, the performance of the classifiers is studied against the number of eigenvectors used to represent the subspace. Fig. 4 shows the performances of the classifiers I-V that are trained and tested on data collected from a single subject. Here, the training is very specific to an individual subject and the performance shown here is also specific to the same subject. It is noted that the accuracy improves as the number of eigenvectors is increased from one to six, which results in a wider span of the artifact subspace of an individual BMA class. However, the performance saturates with further increase in the number of eigenvectors, since this results in overlapping of the spanned subspaces for different classes.

Due to correlation among the eigenfunctions of the specified subclasses, there is a drop in accuracy with increasing number of classes. The peak P_T value for classifier I (4 classes) is 98%, whereas for classifier V (8 classes) $P_T = 85\%$. Thus, it is possible to accurately recognize the BMA from the ambulatory ECG itself, the degree of accuracy depends on separability of the BMAs.

The complete performances of the above BMA classifiers I, II, III and IV are presented in Fig. 5(a)-(d), respectively, showing the confusion matrix for all classes. In all cases six eigenvectors are used for the classification of the data collected from a single subject. In classifier I there are four BMA classes: 1, 2, 3, and 4 (Table II). The accuracy P_T of the classifier I is 98% with a false detection rate $P_F = 1.4\%$. This suggests that all these four classes of BMA are very well separable using PCA-based filtering.

In BMA classifier II, there are five BMA classes: 1, 2, 3a, 3b, and 4. Here, the activities of walking (3a) and climbing down (3b) stairs are recognized as separate classes. However, there is moderate confusion between these two classes: 3a and 3b, as shown in Fig. 5(b), about 18% of total known labels of climbing down stairs are misclassified as walking and 4% of walking labels are misclassified as climbing down stairs. For these two classes, the average $P_T = 90\%$ and $P_F = 8.5\%$. The average

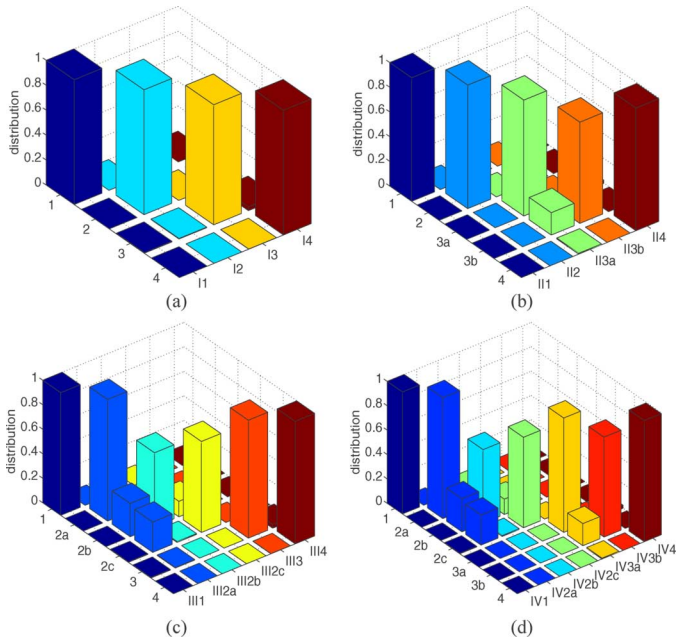

Fig. 5. Confusion matrices for BMA detection for classifiers (a) I, (b) II, (c) III and (d) IV. The horizontal axes in each case represent known and recognized BMA classes.

performance for classifier II is $P_T = 96\%$ and $P_F = 4\%$. Further studies will be required to determine if there is a fundamental limitation in separating walking and climbing down.

In BMA classifier III there are six BMA classes: 1, 2a, 2b, 2c, 3, and 4. Here, the movement of left arm 2a), right arm 2b), and both arms 2c) are recognized as separate classes. However, a significant level of confusion exists between these three classes as shown in Fig. 5(c). On average, 25% of total known labels of both the classes 2b and 2c are misclassified as 2a, and 12% of total known labels of the 2b are misclassified as 2c. For these three classes, average P_T is 77% and P_F is 17%. The average performance for classifier III is $P_T = 91\%$ and $P_F = 7\%$. This suggests that for the given lead-II configuration, any movement of the arms (be it left or right) does affect the ECG signal in a similar manner which reduces the differentiability of the corresponding BMAs.

In BMA classifier IV, there are seven BMA classes: 1, 2a, 2b, 2c, 3a, 3b, and 4. Here, the BMAs 2a) left arm, 2b) right arm, 2c) both arms movement, 3a) walking, and 3b) climbing down stairs are recognized as separate BMA classes. The notable aspect about the classifier IV is that all the seven different BMA classes are recognized by a single classifier. The confusion levels between classes are similar to that of classifier III (arm movements) and classifier II (walking and climbing down stairs). The classifier IV demonstrates $P_T = 88\%$ and $P_F = 10\%$, which is worse than previous cases, due to the large number of classes considered.

In BMA classifier V, there are now eight BMA classes: 1, 2a, 2b, 2c, 3a, 3b, 4, and 5. As compared to the classifier IV, the performance under the BMA subclasses 2a, 2b, and 2c is further deteriorated since BMA 5 also involves arm movement. The classifier V has $P_T = 84\%$ and $P_F = 13\%$.

TABLE III
INTERSUBJECT VARIABILITY OF CLASSIFICATION RATES (IN %) OF THE SINGLE SUBJECT CLASSIFIERS OVER THE ENTIRE SUBJECT POPULATION

Classifier	Accuracy (P_T)		False detection rate (P_F)	
	mean	std. dev.	mean	std. dev.
I	92.44	6.71	5.95	5.38
II	86.81	8.38	9.78	6.64
III	79.85	7.11	15.23	5.52
IV	73.98	8.97	19.06	6.53
V	72.79	7.51	20.20	6.08

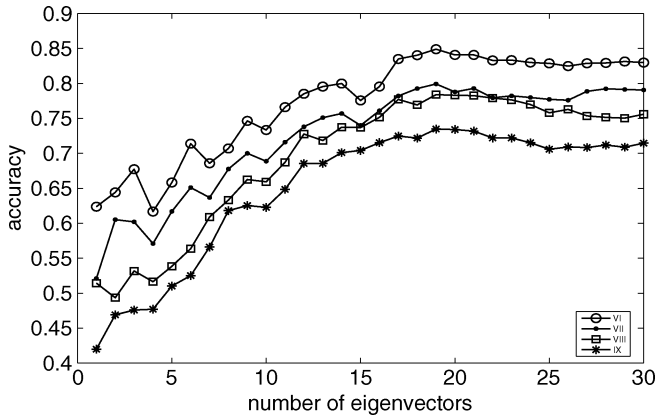

Fig. 6. Accuracy of the combined classifiers as a function of number of eigenvectors used to represent the artifacts when the data is collected from different subjects. Here, the classifiers are VI, VII, VIII and IX.

The results given so far (Fig. 5) correspond to analyzing the performance of the classifiers on a single subject (subject number one in this case). We now compute the intersubject variability of the obtained results by computing the classification rates for each classifier trained and tested on individual subjects. This is given in Table III for the classifiers I-V. It can be seen from the table that the mean accuracy (P_T) and mean false detection rate (P_F) for these classifiers display similar behaviors as discussed earlier. The standard deviation for accuracy is quite low. However, the standard deviation for the false detection rates appears to be on a slightly higher side.

The results presented above were for the classifiers I to V, trained and tested over a single subject. The training over a single subject allowed us to shield the classifier from possible interpersonal variability. Hence, we now repeat the experiments where PCAs are learnt not from an individual subject, but from all subjects available with us. The classifiers VI to IX are trained on 23 different subjects to also understand the impact of interpersonal variability on classifier performance. As mentioned earlier, one-third of the available ECG beats from each subject have been used for training purposes. The accuracy of classification for various choices of the number of eigenvectors is plotted for the classifiers VI to IX in Fig. 6. As compared to the training over a single subject the required number of eigenvectors is much higher and the maximum P_T is only 85%, as expected.

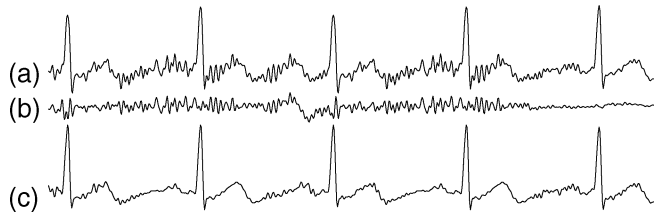

Fig. 7. Illustration of artifact removal from ambulatory ECG using the class specific PCA based filtering. (a) Original ECG signal before any artifact removal, (b) artifact signal derived by the proposed method, and (c) reconstructed ECG signal after subtracting only the artifact signal.

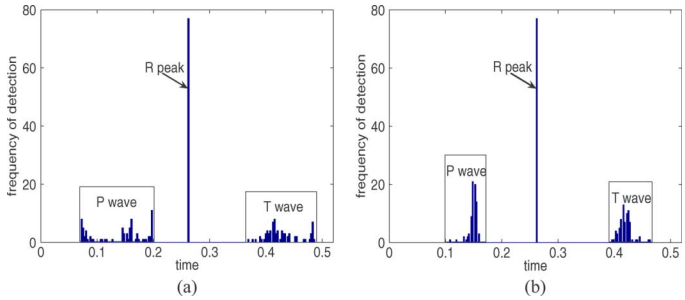

Fig. 8. Histograms of location estimates of P, R, and T waves (a) when motion artifacts were present and (b) after artifact removal. The horizontal axes represents actual time in seconds.

To study further the effect of interpersonal variation in ECG data $(\underline{\eta'})$ the classifier X with four BMA classes 1, 2, 3, and 4 is trained on 22 subjects out of the total 23 subjects, leaving each time one designated test subject. This is equivalent to employing a leave-one-out testing method. The performance of classifier X is $P_T(\max.) = 72\%$ and $P_F(\min.) = 26\%$. Thus, it appeares that the error signal generated due to interpersonal variation $(\underline{\eta'})$ is significant. It is, therefore, advisable that the classifier be customized for a given user in order to achieve the highest accuracy.

B. Detection of P and T Waves in Presence of BMA

Fig. 7(a) shows a sequence of actual ECG beats in presence of BMA (walking) prior to artifact removal. In Fig. 7(b) the component due to motion artifacts as derived by the proposed method using the classifier III is shown. In Fig. 7(c) the reconstructed ECG signal after subtracting the artifact signal is shown. The ECG signal after the removal of motion artifacts is quite clean even though this has been accomplished with a single lead, low cost device.

This artifact removal procedure helps improve the quality of analysis of ECG signal in presence of BMA as demonstrated here in the detection of P and T waves in the collected ECG beat data. The P wave is a small and smooth peak that occurs just before the QRS complex due to atrial activity of the heart and the T wave occurs following the QRS complex due to the ventricular activity. In order to detect the P, QRS complex and T waves, we use a combination of two existing techniques in the literature [11]–[13]. First, the ECG signal is smoothed by a low-pass filter with a 3 dB cutoff at 12 Hz as recommended in [12] for P and T wave detection. Then a morphological based method for detecting P and T waves is applied which is inspired by the method of QRS detection in [13]. Since the R-peak position is in the middle, P and T waves are located by searching for maxima in the appropriate windows before and after the R-peak position in the output of the morphological operation.

The histograms representing the location of P and T waves detected from ECG beats for a single subject shown in Fig. 7, before and after artifact removal, are shown respectively in Fig. 8(a) and (b). It may be noted that since the input beats have already been resampled to have the same number of samples, the samples may correspond to different timings based on the resampling factor used earlier. In order to plot them on an actual time unit, the locations of the detected P and T waves are shown after correcting for the resampling operation. In Fig. 8(a), the histogram without the artifact removal is broadly spread out (standard deviations of 46.4 and 29.8 ms, respectively, for P and T locations) while in Fig. 8(b) the histogram is much narrower (standard deviations of 8 and 11.9 ms, respectively, for P and T locations). This shows that in the presence of BMA induced artifact, the 12 Hz low-pass filter as suggested in [12] alone is not sufficient for the accurate location of P and T waves and the artifact removal improves the quality of analysis.

VI. Conclusion

In this paper we have studied classifiability of various BMA like sitting still, movement of arms, walking and climbing stairs up and down using the motion artifacts present in ECG signals. It is observed that BMAs have different separations between them and this determines the accuracy of classification. For example, while climbing up stairs is recognized with a good accuracy $(P_T = 99\%)$, there exist moderate confusion between walking and climbing down stairs and significant confusion between movement of left, right and both arms. When we merge two overlapping classes such as walking and climbing down stairs into a single BMA class the performance expectedly improves. It would be of interest to study the confusion level if the pace of walking/climbing downstairs is increased. Similarly, confusion levels in the case of vigorous arm movement will be of interest. Currently, we have refrained from such activities that may impose stress on the heart.

The performance is the best when the classifier is trained and tested on a single subject, meaning that personal training is recommended rather than generic training on multiple subjects.

In order to be able to use a PCA-based analysis, we had to resort to resampling of the ECG beats to match the dimensionality, which may introduce certain artifacts in the QRS complex. Another possible option is to do zero padding to match the dimension. However, this would introduce artifacts in the actual BMA signal that is prevalent over the entire beat duration. This issue is being currently investigated.

Further, for the proposed supervised learning technique, the available ground truth is in terms of labels that qualitatively describe activities (e.g. walking gently). However, a more precise labeling of BMAs in terms of speed and rigorousness is likely to provide a better understanding of the impact of the resultant motion artifacts. This may be achieved by attaching a network of motion sensors to the body and recording the motion signal synchronously with the ECG signal. The heart rate and the respiration rate are closely related to body movement, thus, the classification results can be improved further by considering these two

parameters. Finally, our studies have been restricted to dealing with healthy subjects only. The future plan is to study subjects with actual cardiac abnormalities.

ACKNOWLEDGMENT

The authors would like to thank Prof. S. Mukherji, IIT Bombay for his comments. They would also like to acknowledge the constructive reviews that have helped in improving the quality of presentation.

REFERENCES

[1] M. Shojaei-Baghini, R. K. Lal, and D. K. Sharma, "A low-power and compact analog CMOS processing chip for portable ECG recorders," presented at the Asian Solid State Circuit Conference, A-SSCC'05, Hshinchu, Taiwan, Nov. 2005.

[2] V. X. Afonso, W. J. Tompkins, T. Q. Nguyen, and K. Michler, "Comparing stress ECG enhancement algorithms with an introduction to a filter bank based approach," *IEEE Eng. Med. Biol. Mag.*, pp. 37–44, May/Jun. 1996.

[3] V. S. Nimbargi, V. M. Gadre, and S. Mukherji, "Characterization of ECG motion artifacts using wavelet transform and neural networks," presented at the Indian Conference on Medical Informatics and Telemedicine, Kharagpur, West Bengal, India, 2005.

[4] F. Jager, G. B. Moody, and R. G. Mark, "Detection of transient ST segment episodes during ambulatory ECG monitoring," *Comput. Biomed. Res.*, vol. 31, pp. 305–322, 1998.

[5] M. Astrom, J. Garcia, P. Laguna, and L. Sornmo, "ECG based detection of body position changes," *Signal Process. Rep.*, vol. SPR-48, pp. 1–34, Nov. 2000.

[6] J. Garcia, M. Astrom, J. Mendive, P. Laguna, and L. Sornmo, "ECG-based detection of body position changes in ischemia monitoring," *IEEE Trans. Biomed. Eng.*, vol. 50, no. 6, pp. 677–685, Jun. 2003.

[7] L. Sornmo, "Vectorcadiographic loop aignment and morphologic beat-to-beat variability," *IEEE Trans. Biomed. Eng.*, vol. 45, no. 12, pp. 1401–1413, Dec. 1998.

[8] J. Bartosik, O. Pahlm, L. Edenbrandt, J. Svensson, W. K. Haisty, and G. S. Wagner, "Reconstruction of the standard 12-lead ECG from recordings using nonstandard activity-compatible proximal limb lead positions," *J. Electrocardiol.*, vol. 28, no. 1, pp. 33–38, 1995.

[9] F. Jager, R. Mark, and G. Moody, "Analysis of transient ST segment changes during ambulatory monitoring," in *Computers in Cardiology*. Los Alamitos, CA: IEEE Computer Soc., 1991, pp. 453–456.

[10] J. Pan and W. L. Tompkins, "A real-time QRS detection algorithm," *IEEE Trans. Biomed. Eng.*, vol. 32, no. 3, pp. 230–236, Mar. 1985.

[11] B.-U. Kohler, C. Hennig, and R. Orglmeister, "The principles of software QRS detection," *IEEE Eng. Med. Biol.*, pp. 42–57, Jan.–Feb. 2002.

[12] P. Laguna, R. Jane, and P. Caminal, "Automatic detection of wave boundaries in multilead ECG signals: Validation with the CSE database," *Comput. Biomed. Res.*, vol. 27, no. 1, pp. 45–60, 1994.

[13] P. E. Trahanias, "An approach to QRS complex detection using mathematical morphology," *IEEE Trans. Biomed. Eng.*, vol. 40, no. 2, pp. 201–205, Feb. 1993.

Tanmay Pawar was born in Jobat, India. He received the B.E. degree in electronics and communication engineering from the Dharmasinh Desai Institute of Technology, Nadiad, India, in 1996. He received the M.Tech. degree in electrical engineering from the Indian Institute of Technology, Bombay, in 2002 where he is currently working towards the Ph.D. degree.

He joined the Birla Vishvakarma Mahavidyalaya Engineering College, Vallabh Vidyanagar, India, in 1997 as a Lecturer and is currently serving as an Assistant Professor. His areas of research interest include biomedical signal analysis and pattern recognition.

Subhasis Chaudhuri (S'86–M'87–SM'02) was born in Bahutali, India. He received the B.Tech. degree in electronics and electrical communication engineering from the Indian Institute of Technology (IIT), Kharagpur, in 1985. He received the M.S. and the Ph.D. degrees, both in Electrical Engineering, from the University of Calgary, Calgary, AB, Canada, and the University of California, San Diego, respectively.

He joined the IIT, Bombay in 1990 as an Assistant Professor and is currently serving as Professor and Head of the Department. He has also served as a Visiting Professor at the University of Erlangen-Nuremberg, Erlangen, Germany, and the University of Paris XI, Paris, France. He is the coauthor of the books *Depth From Defocus: A Real Aperture Imaging Approach* (Springer, 1998), and *Motion-Free super-Resolution* (Springer, 2005). He has also edited *Super-Resolution Imaging* (Kluwer, 2001). His research interests include image processing, computer vision, and multimedia.

Dr. Chaudhuri is a fellow of the Alexander von Humboldt Foundation, Germany, Indian National Academy of Engineering, Indian Academy of Sciences, and the IETE, India. He is the recipient of Dr. Vikram Sarabhai Research Award for the year 2001, the *Swarnajayanti Fellowship* in 2003, and the S. S. Bhatnagar Award in engineering sciences in 2004.

Siddhartha P. Duttagupta (M'04) received the B.Tech. degree in electronics and electrical communication engineering from the Indian Institute of Technology (IIT), Kharagpur in 1991. He received the M.S. and the Ph.D. degrees, both in electrical engineering, from the University of Rochester, Rochester, NY, in 1992 and 1998, respectively.

He joined the IIT, Bombay in 2002 as an Assistant Professor. Previously, he was the Director of Technology, Solar Integrated Technologies, Los Angeles, CA. His research interests include nanoelectronics, electronics reliability and renewable energy.

Dr. Duttagupta has published more than 40 peer reviewed articles.